Computational Microstructural Optimization Design Tool for High Temperature Structural Materials

Rajiv S. Mishra (PI), Aniket Dutt (PhD student)
University of North Texas
Indrajit Charit (co-PI), Somayeh Pasebani (PhD student)
University of Idaho

Project Manager: Dr. Richard Dunst
Grant Number: DE-FE0008648
Performance Period: Sep. 2012 to Aug. 2014

2014 NETL Crosscutting Research Review Meeting
Pittsburgh, May 20, 2014

Objectives

- Develop a methodology for microstructural optimization of alloys - genetic algorithm approach for alloy microstructural optimization using theoretical models based on fundamental micro-mechanisms, and
- Develop a new computationally designed Ni-Cr alloy for coal-fired power plant applications.

Robert R. Romanosky, National Energy Technology Laboratory, April 2012

Materials Limit the Current Technology

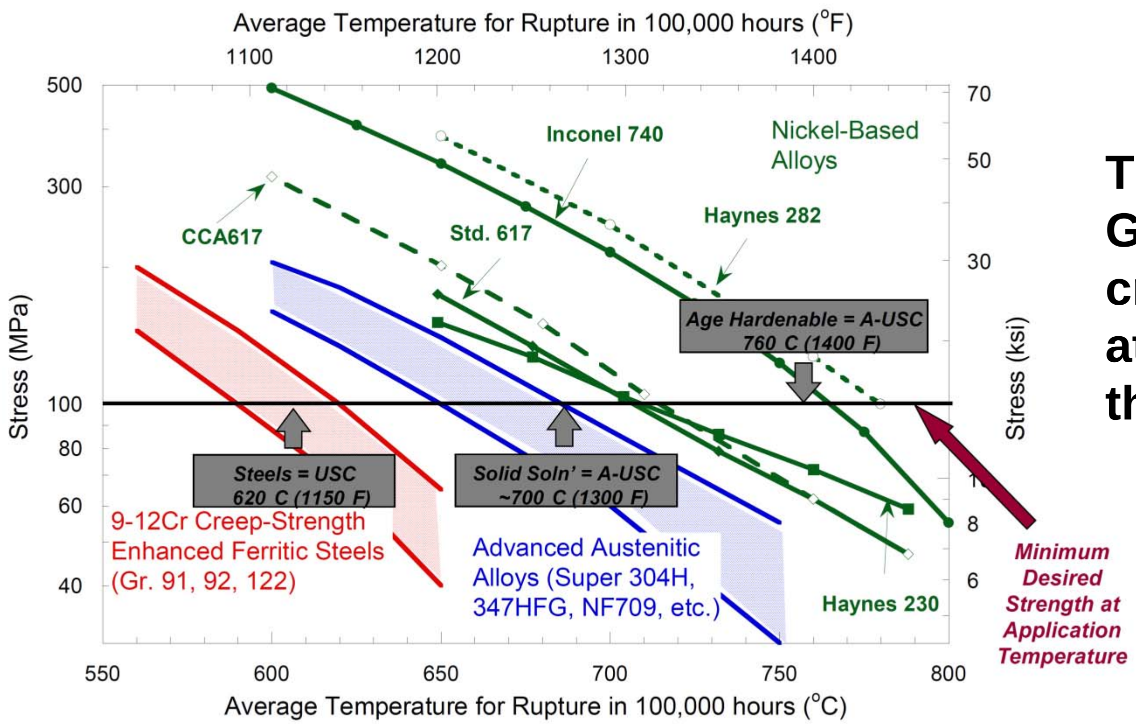

This translates into a GOAL of minimum creep rate <2.7×10^{-9} s^{-1} at 100 MPa at 800 °C for this project

Background – A Bit of History

Timeline of dislocation-particle strengthening

- Dispersion strengthening identified as a potent mechanism for enhancing elevated temperature strength in the early works of Ansell and Weertman in 1950s
  - CONCEPT- Elastically hard particle repels dislocation
- Srolovitz and co-workers in 1980s
  - FUNDAMENTAL SHIFT- dislocation-particle interaction undergoes repulsive→attractive transition at elevated temperatures >0.35 T_m

Background - RECAP

Summary of some of the key development made possible by TEM studies

Reference	Remarks
Nardone and Tien (1993)	First identification of departure side pinning.
Schroder and Arzt (1985)	Weak-beam micrographs showing clear dislocation contrast at the dispersoid.
Herrick et al. (1988)	First quantification of (a) percentage dislocation looped vs. attached, and (b) critical take-off angle as a function of temperature.
Liu and Cowley (1993)	Multiple dislocation-particle interaction; sharp kinks on the detached dislocations that straighten out.

A dispersion strengthened platinum alloy
(Heilmaier *et al.* 1999)

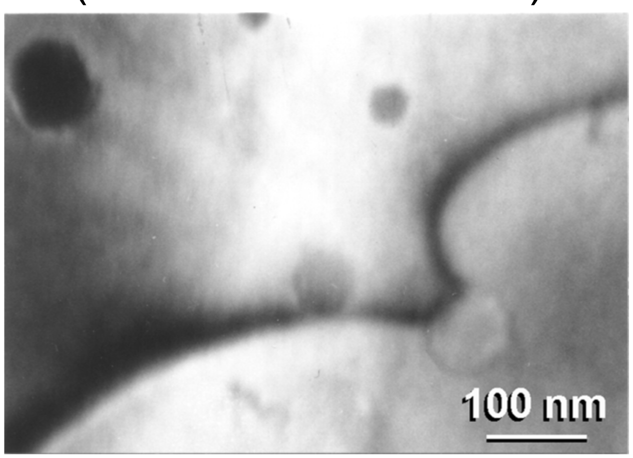

Al-5 wt.% Ti alloy
(Mishra and Mukherjee 1995)

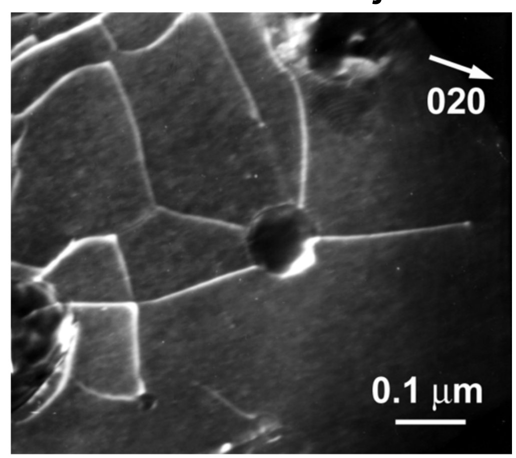

Background – Theoretical Models

Development of dissociation and positive climb concepts

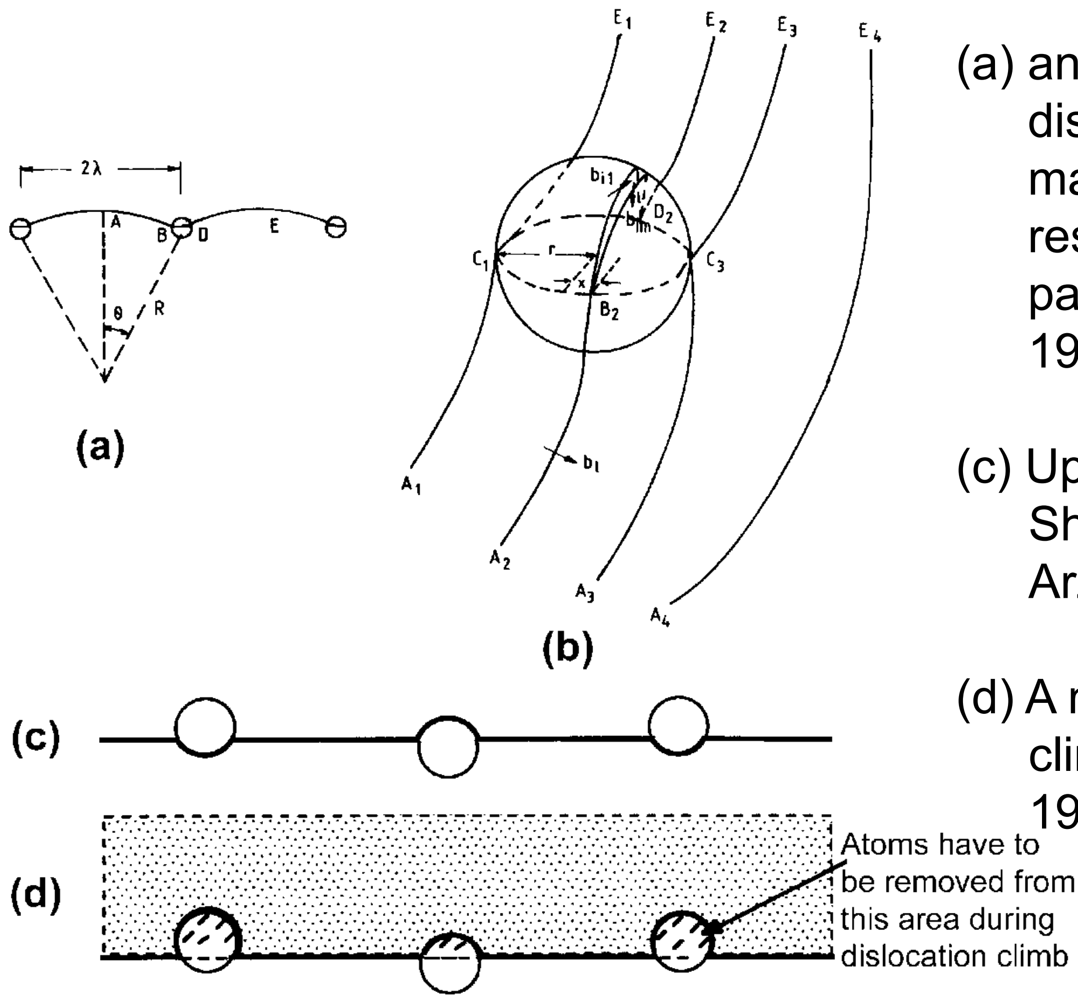

(a) and (b) A schematic illustration of dissociation of dislocation at matrix-particle interface that can result in an attractive dislocation-particle interaction (Mishra et al. 1994).

(c) Up and down climb concept of Shewfelt and Brown (1977) and Arzt and Ashby (1982).

(d) A modified concept of ‘positive climb’ (Mishra and Mukherjee 1995).

Discussion of Strengthening Mechanisms

There are four major components to strengthening in the nanostructured nickel based alloys produced by mechanical alloying:

- grain boundary strengthening,
- solid solution strengthening
- dispersion strengthening, and
- composite strengthening.

Effect of temperature

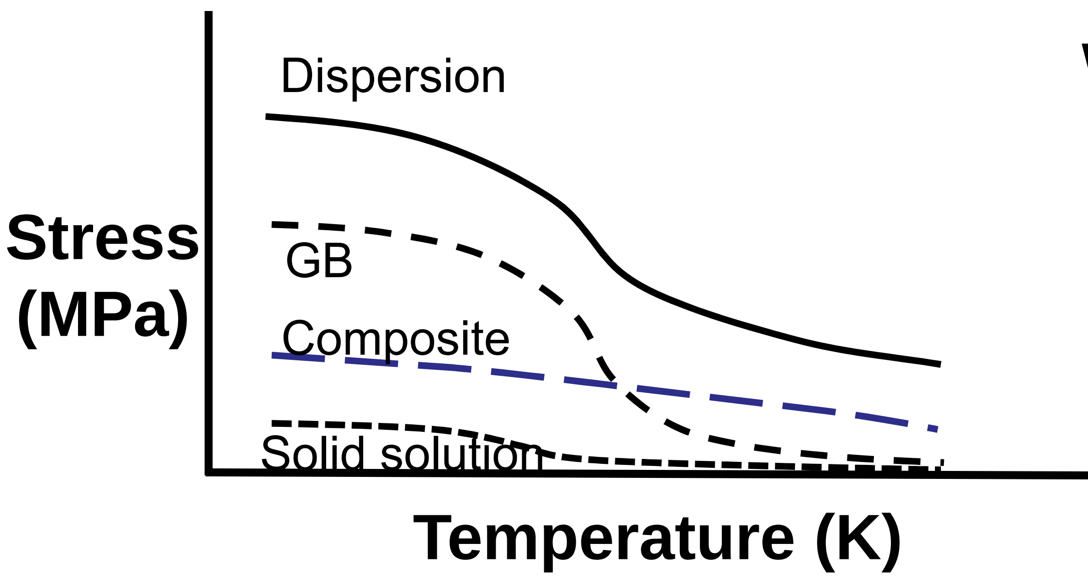

What are the additivity rules?

$$\sigma_{alloy} = \Sigma \sigma_i$$

$$\sigma_{alloy} = \sqrt{\Sigma (\sigma_i)^2}$$

$$(\sigma_{alloy})^k = \Sigma \sigma_i^{\,k}$$

Proposed Microstructure

Develop dual-scale strengthened Ni-Cr-Al_2O_3 alloys
The chosen alloy system has:

- Cr for solid solution strengthening
- nano Cr_2O_3 and/or CrN particles of 2-3 nm diameter for dispersion (currently using nano-Y_2O_3) strengthening
- submicron Al_2O_3 of 0.5-1 micron diameter for composite strengthening through increase in modulus

What is the level of synergy?

- Does the load transfer effectively enhance the creep life for equiaxed reinforcement?

Overview of This Project

OBJ1: Microstructural Optimization

1A. Definition of design goals (UNT-UI-NETL) and material parameter constraints (UNT)
Strength, ductility, creep, residual stresses

1B. Identification of theoretical and phenomenological models (UNT)
Theoretical equations, data sets, empirical relationships

1C. Development of Genetic Algorithm optimization scheme (UNT)
Fitness function, Pareto-optimal solution sets, computational parameters

1D. Computer Simulation of Dislocation Motion for Visualization (UNT)
Multiple obstacles, particle size, particle shape, particle distribution

OBJ2: Develop Ni-Cr-Al_2O_3 with Dual-Scale Microstructure

2A. Processing of GA optimized material (UI)
Milling, degassing and compaction, forging

2B. Experimental validation: Microstructure and Mechanical Properties (UNT and UI)
SEM, TEM, X-ray, hardness, tensile, creep

OUTCOME: Integrated Approach for 'Materials by Design'

Computational part

Strengthening Mechanisms

Ni-Cr ODS alloy

Low T strengthening

- Grain boundary Strengthening
- Dispersion strengthening
- Solid solution strengthening
- Composite Strengthening

High T strengthening

- Dislocation-particle interaction
- Load transfer (reinforcement)

Low temperature strength

Strengthening mechanism	Equation
Grain size strengthening	$\sigma_y = \sigma_0 + Kd^{-0.5}$
Solid solution strengthening	$\Delta\sigma_s = \left(\sum k_i^{\frac{1}{n}} c_i\right)^n$
Dispersion strengthening	$\Delta\sigma_p = \frac{Gb\sqrt{f_d}}{d_p}$
Composite strengthening Load transfer coefficient	$\sigma_c = V_p\sigma_p + V_m\sigma_m$ $\Lambda \approx 1 + 2\left(2 + \frac{l}{R}\right) f_r^{\frac{3}{2}}$

High Temperature strength

Dislocation creep

Modified power law creep [1]

$$\dot{\varepsilon} = 8.3 * 10^8 \frac{DGb}{k_B T}\left[exp\left(-104\sqrt{\frac{b}{\lambda}}\right)\right]\left(\frac{\sigma' - \sigma_0}{E}\right)^5$$

$$\sigma' = \sigma/\wedge$$

Threshold stress

Dissociation and positive climb model [2]

$$\sigma_0 = 0.002\, G\left(\frac{b}{r}\right) exp\left(20\frac{r}{\lambda}\right)$$

1. R. S. Mishra and A. K. Mukherjee, Light weight alloys for aerospace application III, TMS, (1995), 319
2. R.S. Mishra *et al*., Philosophical Magazine A,1994, 69 (6), 1097-1109

GA optimization work

Cost function

$$J = \frac{\left[\sum_{i=S,D,HTS} w_i \left|\left(\frac{P_i}{(P_i)_{desired}}\right) - 1\right|\right]}{n}$$

Various considerations were taken in order to minimize the cost function:

- 100 Individuals were considered in each generation.
- Rank scales were used for the fitness scaling. The rank of the fittest individual was 1, the next fittest was 2 and so on.
- Different methods were used as a selection function to choose parents for the next generation.
- 10 best individuals survived to the next generation.
- Probability of crossover was chosen 0.85 and rest were produce via mutation.
- The optimization was running until 100 generations were completed or the cost function did not vary significant for 25 successive generations.

UNT UNIVERSITY OF NORTH TEXAS Discover the power of ideas.

CFSP Center for Friction Stir Processing

Notation used for variables:

- $[w_S\ w_D\ w_{HTS}]$= Weight factors for low temperature strength, ductility and high temperature strength properties.
- r (nm) is the radius of dispersoids.
- $r1$(nm) and $r2$(nm) are radius of two different dispersoids.
- r_f (nm) is the radius of reinforced particles.
- f_r (%) is volume fraction of reinforcement.
- f_d (%) is volume fraction of dispersoids.
- f_d1(%) and f_d2(%) are the volume fraction of two different dispersoids.

Optimization conditions:

I: 15 nm ≤ r ≤ 20 nm , 300 nm ≤ r_f ≤ 400 nm , f_r ≤ 15 %, T=1073 K, $\dot{\varepsilon} = 10^{-9}\ s^{-1}$

II:10 nm ≤ r1 ≤ 100 nm,1 nm ≤ r2 ≤ 3 nm, 400 nm ≤ r_f ≤ 1000 nm , f_r ≤ 15 %, T=1073 K, $\dot{\varepsilon} = 10^{-9}\ s^{-1}$

III: 1 nm ≤ r ≤ 30 nm , 100 nm ≤ r_f ≤ 1000 nm, f_r ≤ 15 %, T=1073 K, $\dot{\varepsilon} = 10^{-9}\ s^{-1}$

IV:10 nm ≤ r1 ≤ 100 nm,1 nm ≤ r2 ≤ 3 nm, 400 nm ≤ r_f ≤ 1000 nm , f_r ≤ 15 %, T=1073 K, $\dot{\varepsilon} = 10^{-9}\ s^{-1}$

GA results

Condition IV:10 nm ≤ r1 ≤ 100 nm,1 nm ≤ r2 ≤ 3 nm, 400 nm ≤ r_f ≤ 1000 nm, f_r ≤ 15 %, T=1073 K, $\dot{\varepsilon} = 10^{-9}\ s^{-1}$

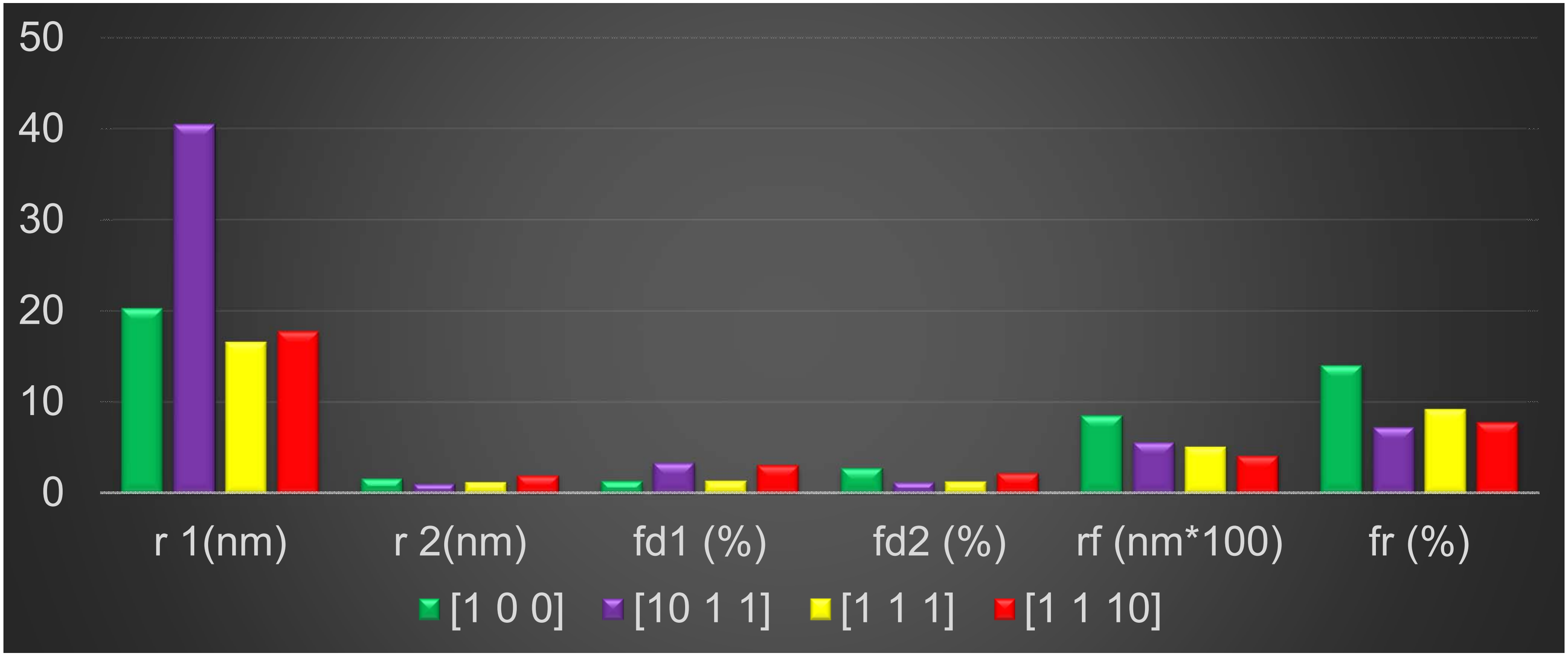

GA operator	Selection	Crossover	Mutation
	Tournament	Arithmetic	Adaptive feasible

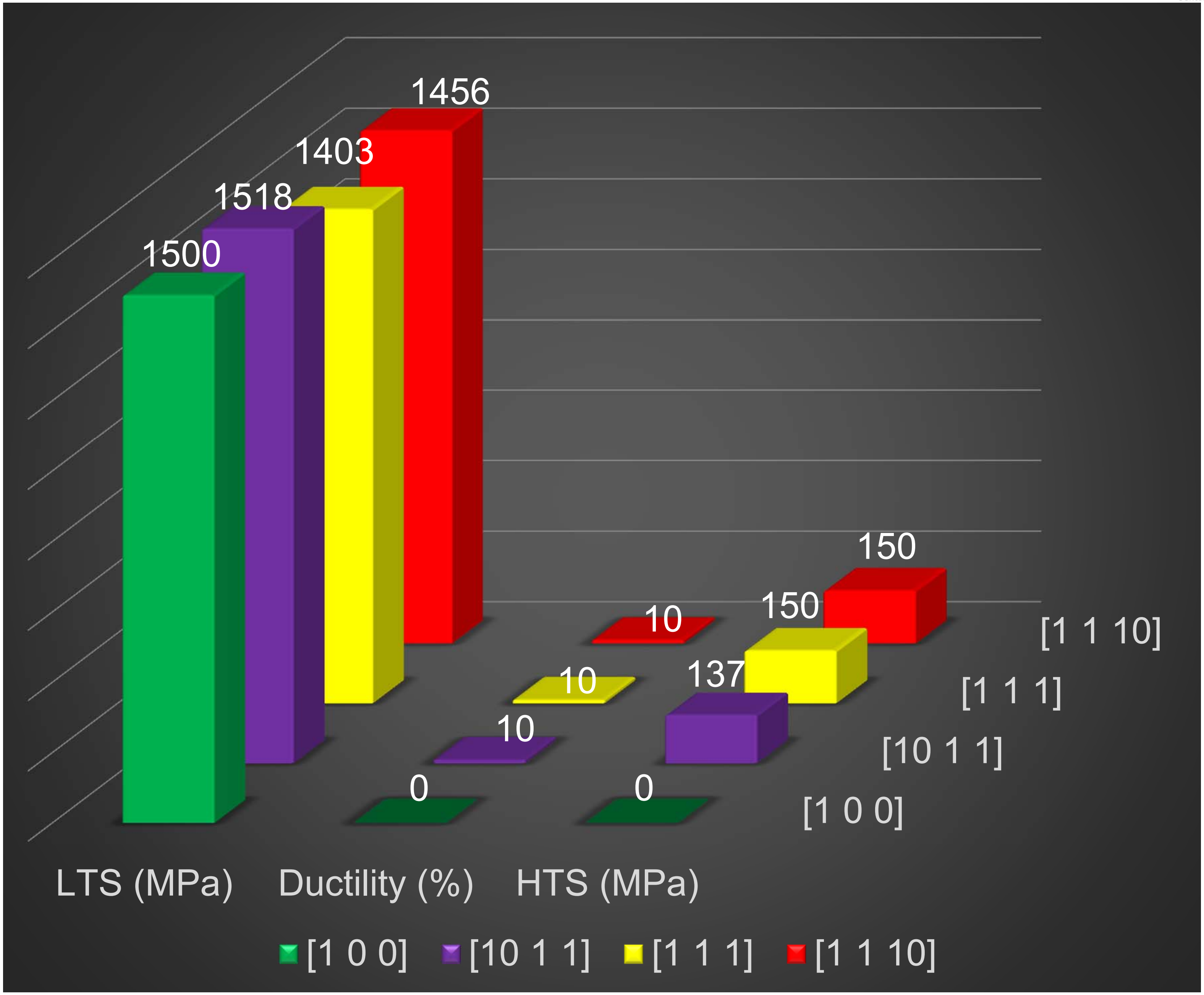
1456
1403
1518
1500
10
150
150
10
137
10
0
0
[1 1 10]
[1 1 1]
[10 1 1]
[1 0 0]
LTS (MPa)
Ductility (%)
HTS (MPa)
[1 0 0]
[10 1 1]
[1 1 1]
[1 1 10]

Summary for computational part

- The optimized results showed:

Condition I	Dispersoids radius (nm) ~ 15
	LTS (MPa) ~ 700
	HTS (MPa) ~ 40
Condition II	Dispersoids radii (nm) ~ 16, 2
	LTS (MPa) ~ 1200
	HTS (MPa) ~ 150
Condition III	Dispersoids radius (nm) ~ 2.5
	LTS (MPa) ~ 1373
	HTS (MPa) ~ 150
Condition IV	Dispersoids radii (nm) ~ 18, 2
	LTS (MPa) ~ 1456
	HTS (MPa) ~ 150

Experimental Part

- Develop fundamental understanding of microstructural characteristics and mechanical properties of the SPSed
    - Ni-20Cr,
    - Ni-20Cr-1.2Y_2O_3, and
    - Ni-20Cr-1.2Y_2O_3-5Al_2O_3 (wt%) alloys

Spark Plasma Sintering

- Hot Uniaxial Pressing with Joule heating by pulsed current
- Particle cleansing effect
- Metal or ceramic powder poured into dies (usually graphite)
- Rapid heating rates
- Near fully dense materials in as short as 5 min
- No texture or extrusion anisotropy
- Two dominant theories of SPS mechanisms
  - Plasma generation
  - Field theories

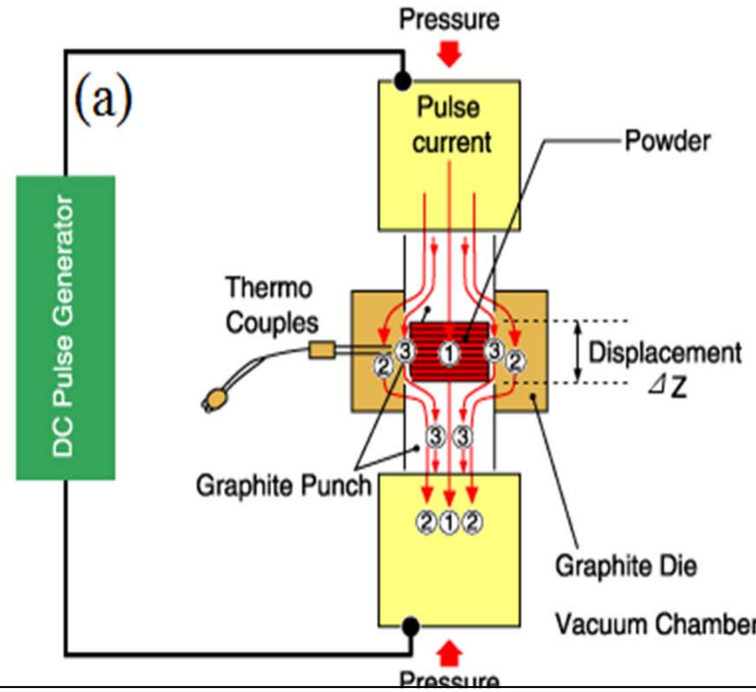

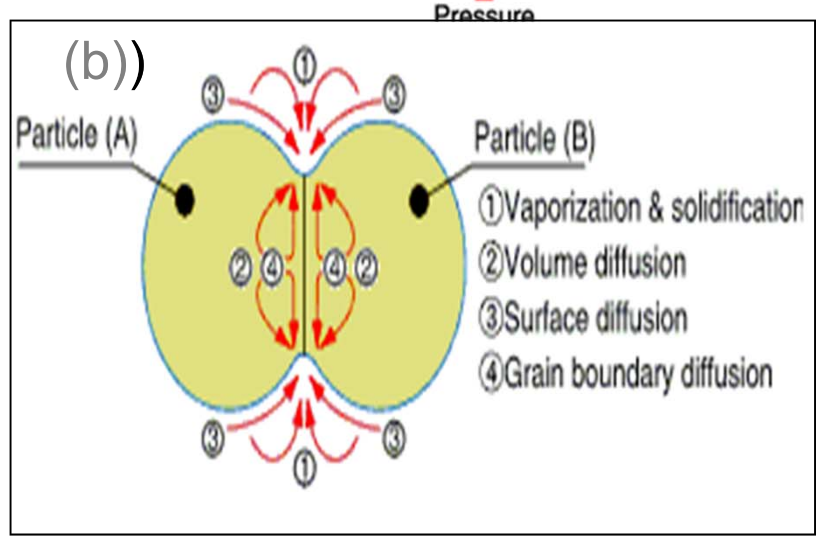

(*M. Suárez et al., 2013*)

Experimental – Spark Plasma Sintering

- Dr. Sinter 515S machine at the Center for Advanced Energy Studies (CAES), Idaho Falls
- Heating rate: 100 ^{o}C/min; applied presssure: ~80 MPa
- An intermediate 15 min dwell at 450 ^{o}C for 15 min (with 4.5 kN applied force) to remove the stearic acid
- Temperatures: 600 / 900 / 1000 / 1100 ^{o}C; dwell time: 5 and 30 min

Spark Plasma Sintering Machine

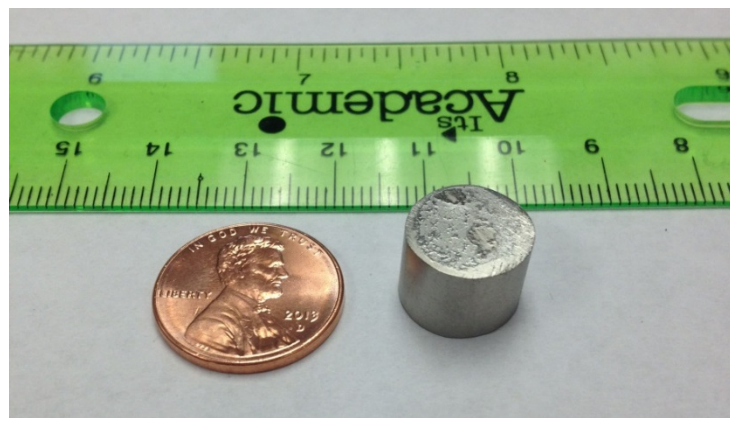

Spark Plasma Sintered Ni-20Cr-1.2Y_2O_3 Alloy

Microstructure – Ball Milled Powder

Ni-20Cr-1.2Y_2O_3 alloy

Milling Time (h)	Crystallite Size (nm)	Lattice Strain (%)	Lattice Constant (nm)	Mean Powder Size (µm)
0	44±12	0.03±0.001	0.3530±0.0002	23.6±1.1
1	17±9	0.03±0.001	0.3532±0.0003	39.2±2.2
2	14±7	0.03±0.001	0.3536±0.0003	33.6±1.5
4	4±2	0.15±0.003	0.3560±0.0004	39.4±3.1

Microstructural parameters quantified by XRD and SEM

Microstructure – Ball Milled Powder

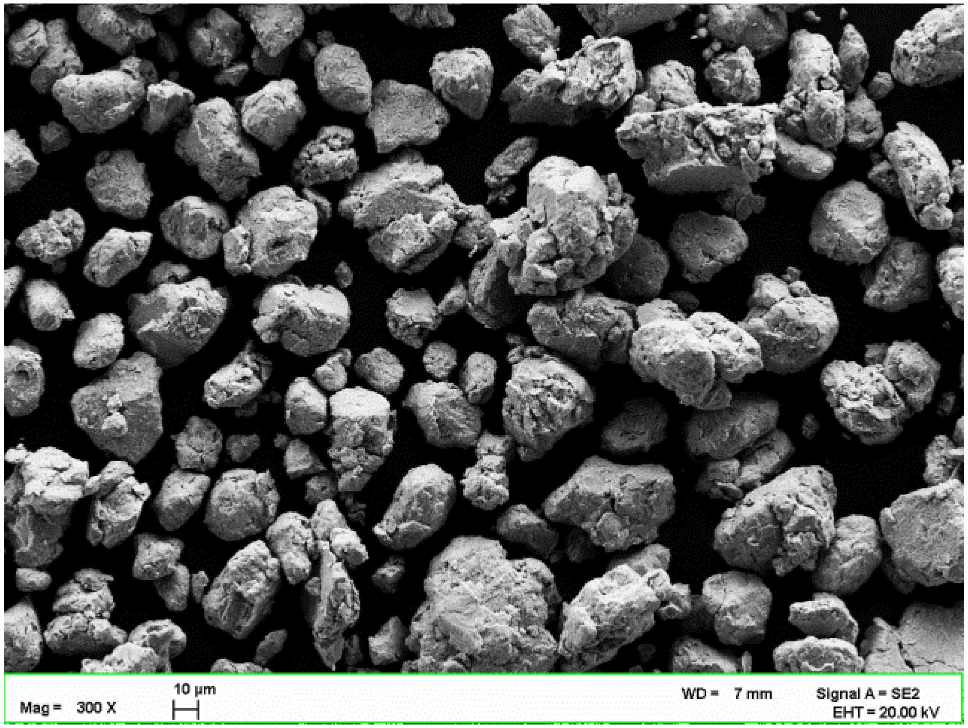

A SEM micrograph of the ball milled (2) Ni-20Cr-1.2Y_2O_3 powder

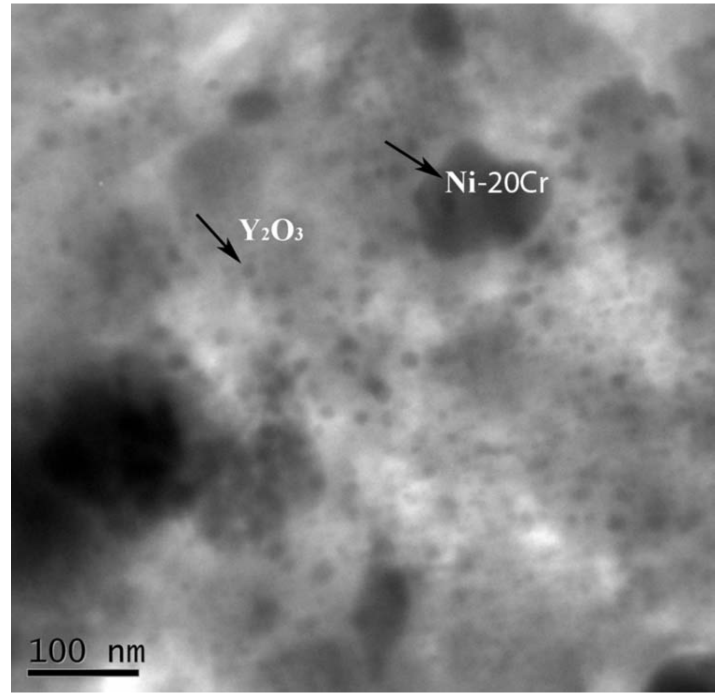

A TEM micrograph of ball milled (2 h) Ni-20Cr-1.2Y_2O_3 powder

- Ni-20Cr-1.2Y_2O_3 : Avg. powder size - 34 µm; crystallite size - 14 nm
- Ni-20Cr: Avg. powder size - 40 µm ; crystallite size: 92 nm

Microstructure of SPSed Alloys

SPS condition: 1100 °C / 30 min

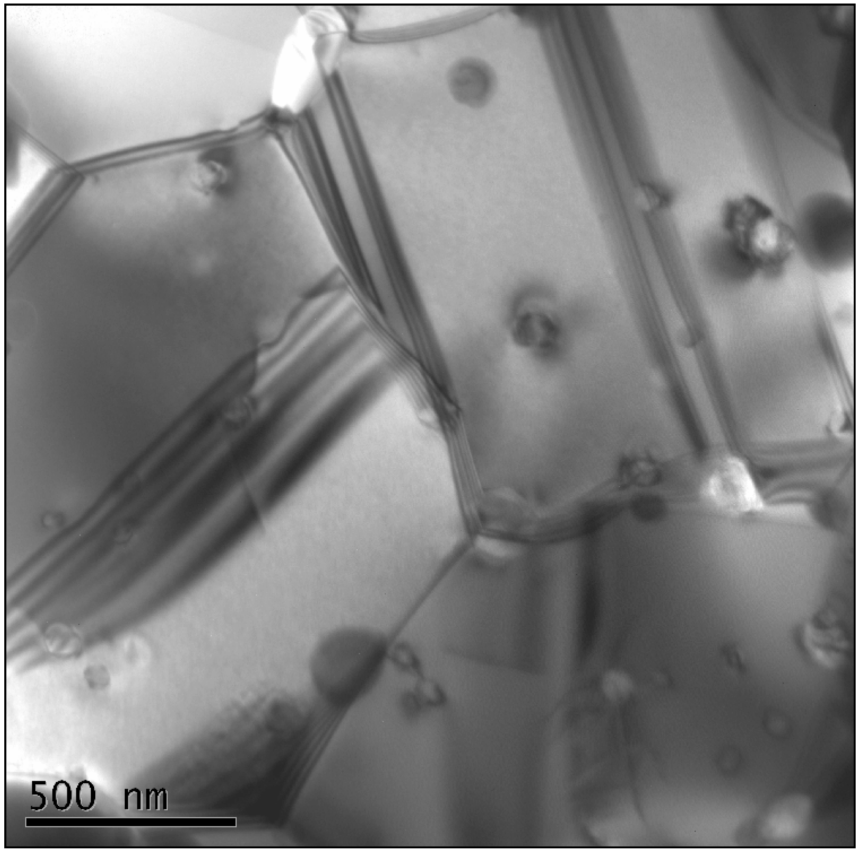

SPSed Ni-20Cr alloy

Avg. Grain size: 630 nm

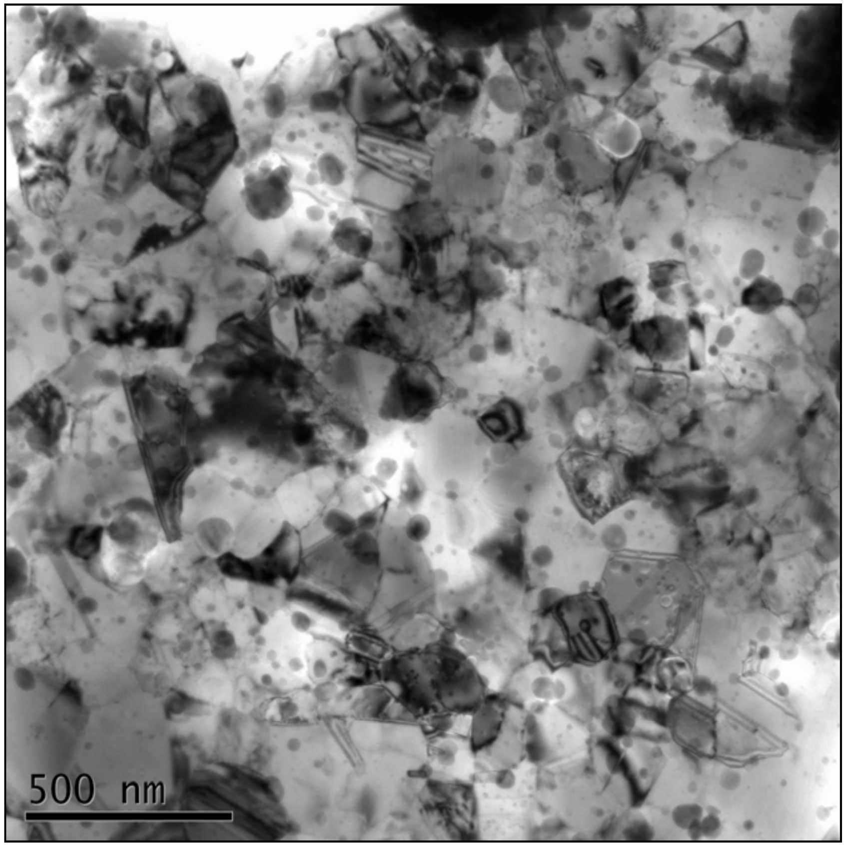

SPSed Ni-20Cr-1.2Y_2O_3 alloy

Avg. Grain size: 130 nm

Particle Compositions – SPSed Alloys

SPS condition: 1100 ^{o}C / 30 min

Ni-20Cr-1.2Y_2O_3 alloy

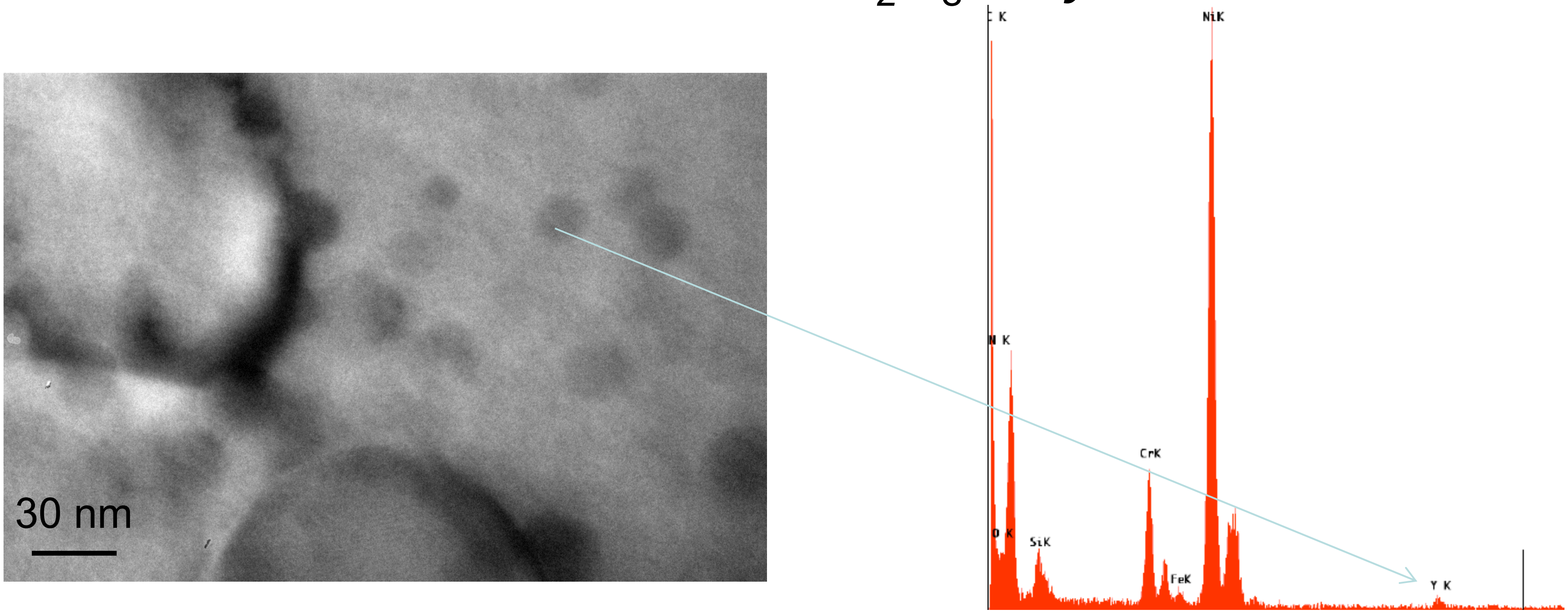

- Three main oxide particle categories in terms of their size:
  - Ni-based oxide in the range of 80-100 nm
  - Cr-based oxide in the range of 20-60 nm
  - Y-based oxide smaller than <15 nm

Microstructure of SPSed Alloys

Milled for 4 hours - SPS condition: 1100 °C / 30 min
Ni-20Cr-1.2Y_2O_3 alloy

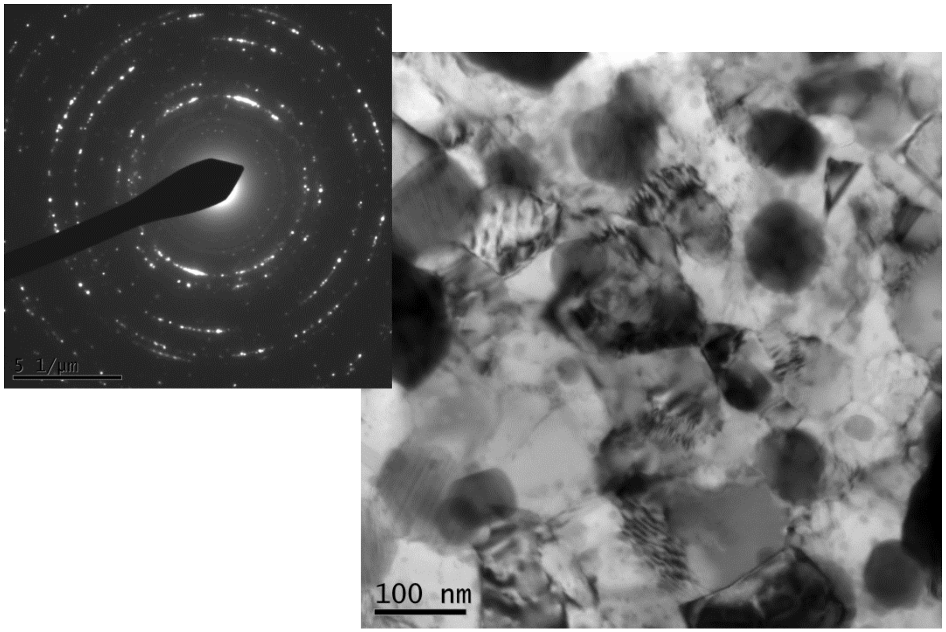

Smaller grain region

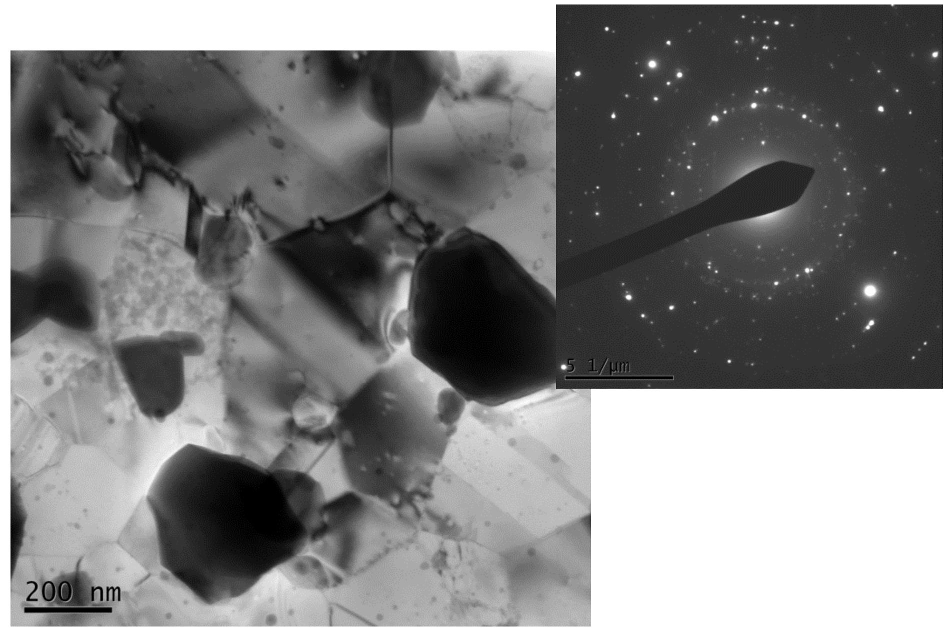

Larger grain region

- With increasing milling time from 2 to 4 hours, there is a tendency to develop bimodal grain size distribution.
- Possibly a higher amount of yttria dissolved in the Ni-Cr matrix.

Microstructure of SPSed Alloys

Milled for 2 hours / SPS condition: 1100 ^oC / 30 min

Ni-20Cr-1.2Y_2O_3-5Al_2O_3 alloy

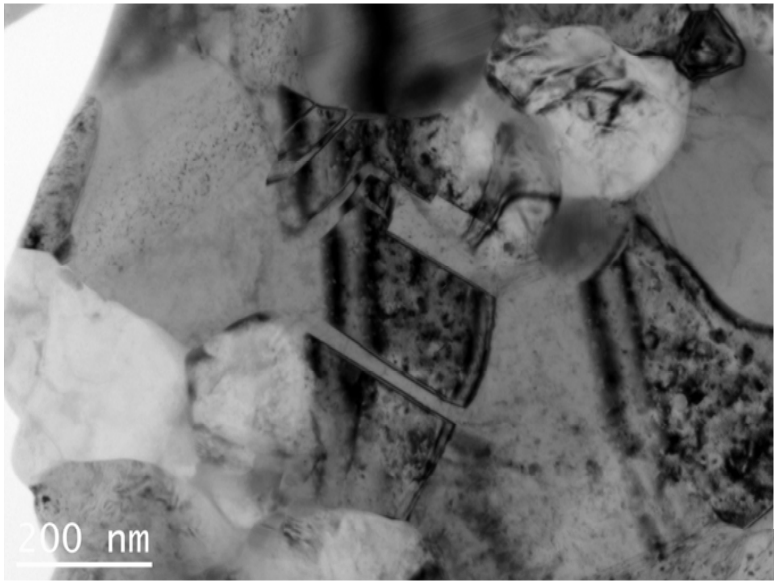

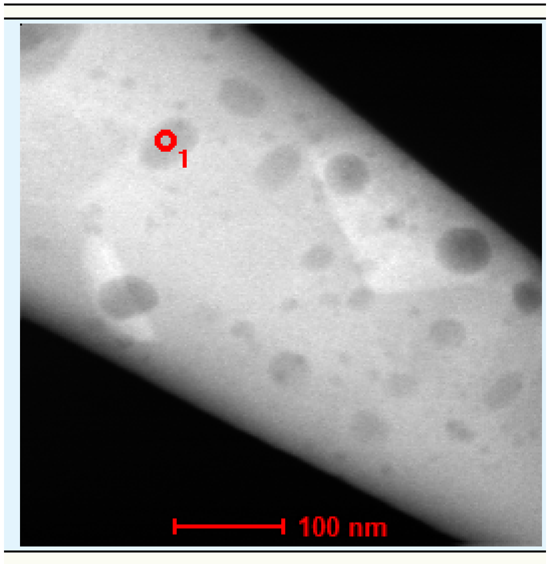

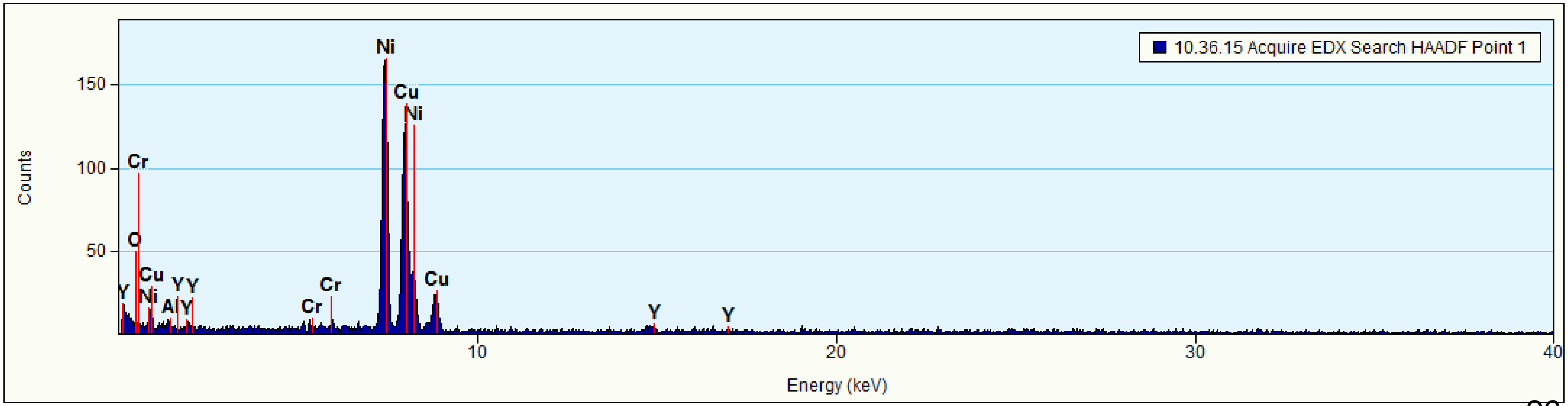

Density and Microhardness - SPS

Powder milled for 2 h, BPR of 10 and ball diameter of 5 mm

Alloy Comp. (wt.%)	SPS parameters	Density (g/cm^3)	Relative Density (%)	Hardness (HV)
Ni-20Cr	1100 ^{o}C / 30 min	8.19	98.95±0.03	201.6±6.2
Ni-20Cr-1.2Y_2O_3	900 ^{o}C / 5 min	7.71	93.93±0.03	395.1±11.4
Ni-20Cr-1.2Y_2O_3	600 ^{o}C / 5 min	5.92	72.19±0.24	130.8±31.9
Ni-20Cr-1.2Y_2O_3	1000 ^{o}C / 5 min	8.15	99.26±0.30	555.9±4.6
Ni-20Cr-1.2Y_2O_3	1100 ^{o}C / 5 min	8.16	99.48±0.05	469.6±7.8
Ni-20Cr-1.2Y_2O_3	1100 ^{o}C / 30 min	8.17	99.55±0.04	471.6±7.5
Ni-20Cr-1.2Y_2O_3-5Al_2O_3	**1100 ^{o}C / 30 min**	**7.7**	**99.18±0.02**	**505.5±10.3**

Nano-indentation of Ni-ODS alloys

Sample	NiCr	NiCr-Y_2O_3-Al_2O_3
Elastic modulus (GPa)	170	249

Compression Test Results

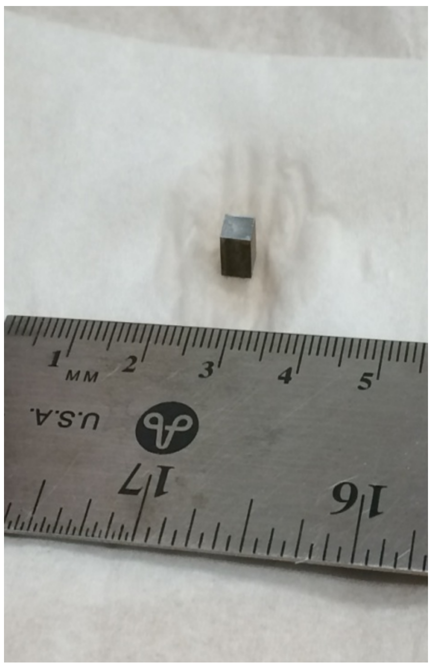

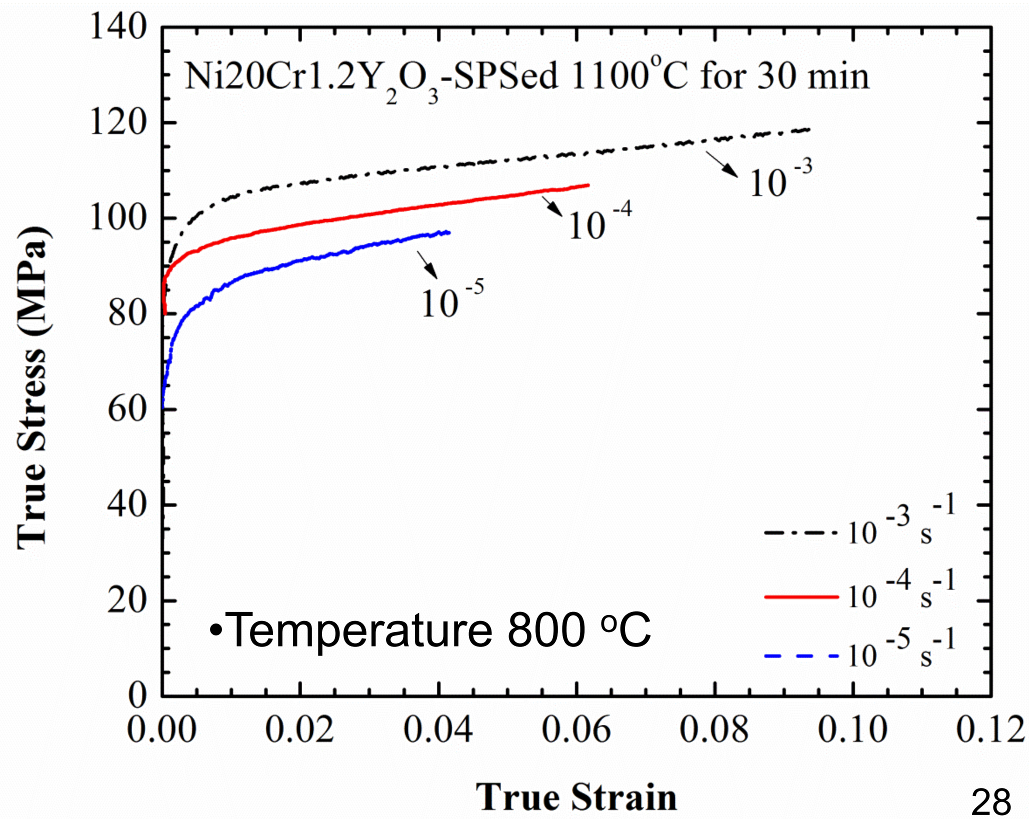

Creep test of NiCr

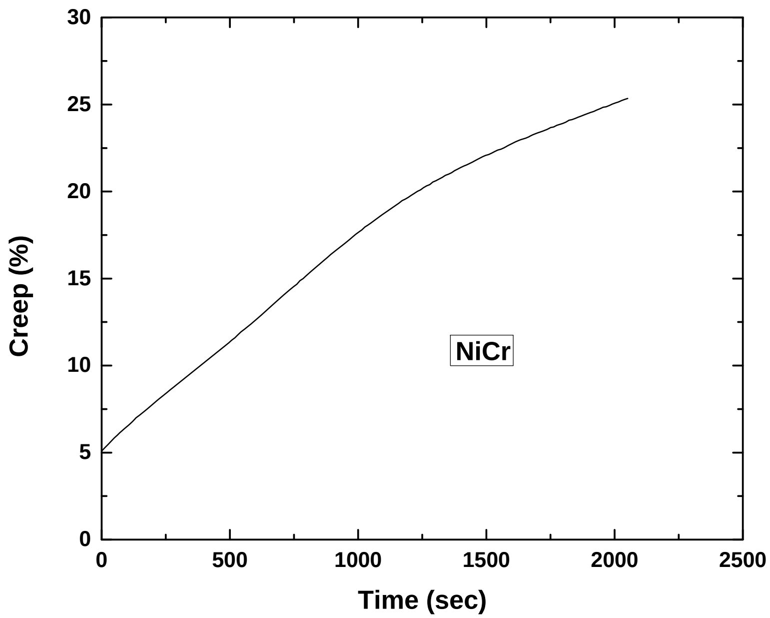

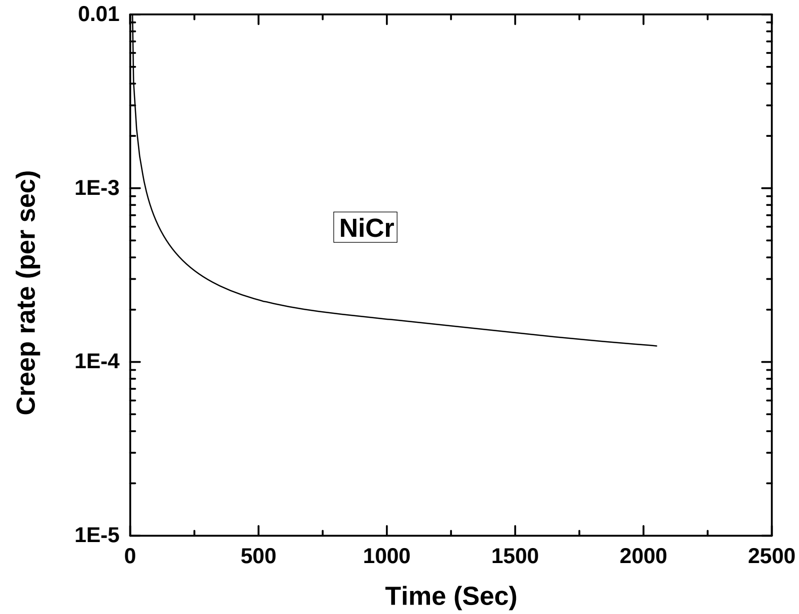

Specimen dimensions (mm*mm*mm)	Stress applied (MPa)	Testing temperature (ºC)
(6.09) * (5.70)* (4.30)	100	800

Minimum creep rate (s^{-1}): 10^{-4}

Creep test of NiCr-Y_2O_3

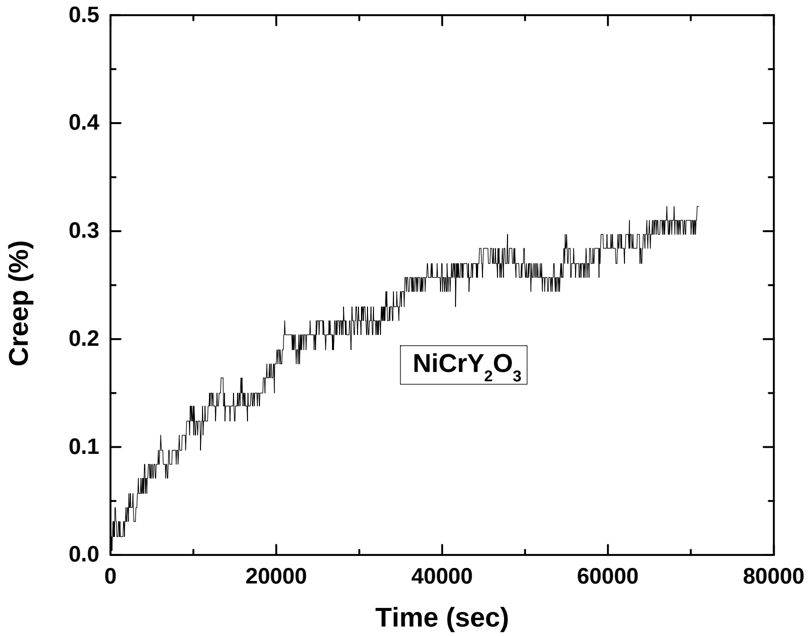

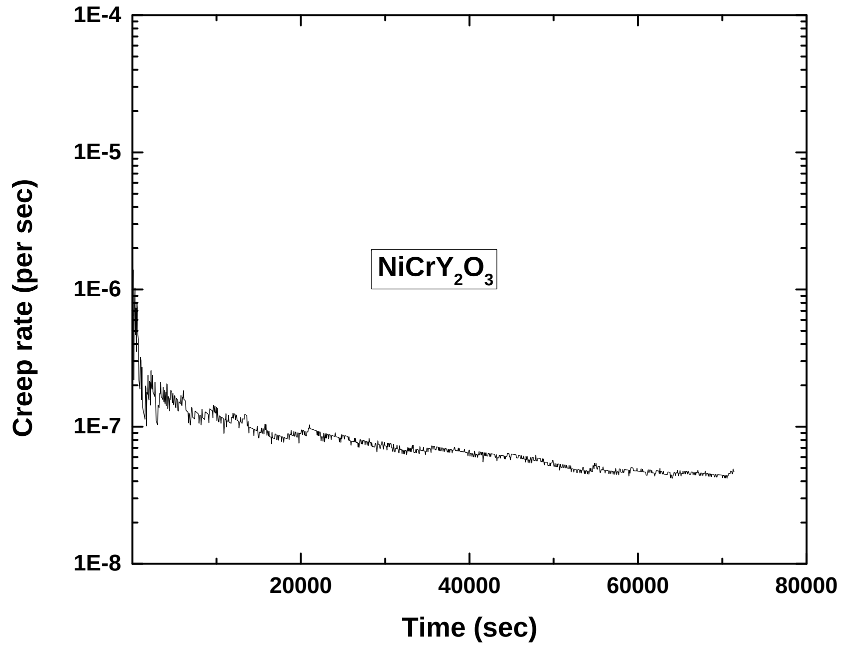

Specimen dimensions (mm*mm*mm)	Stress applied (MPa)	Testing temperature (^oC)
(9.97) * (3.76)* (3.77)	100	800

Minimum creep rate (s^{-1}): $4.7*10^{-8}$

Creep test of NiCr-Y_2O_3-Al_2O_3

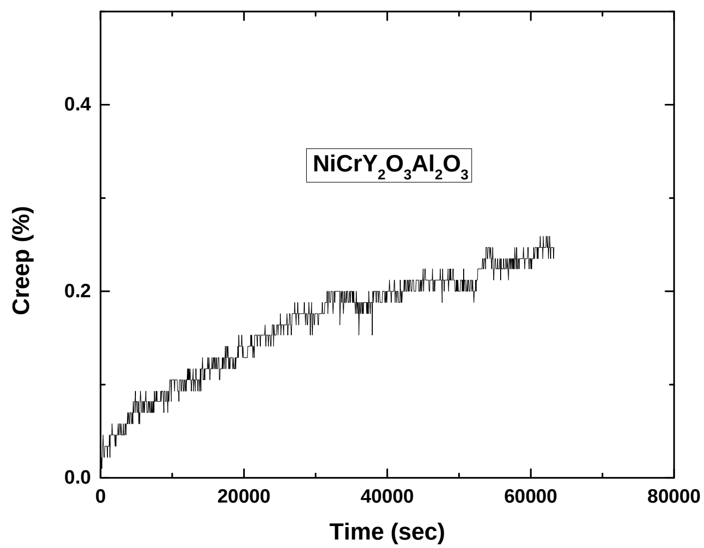

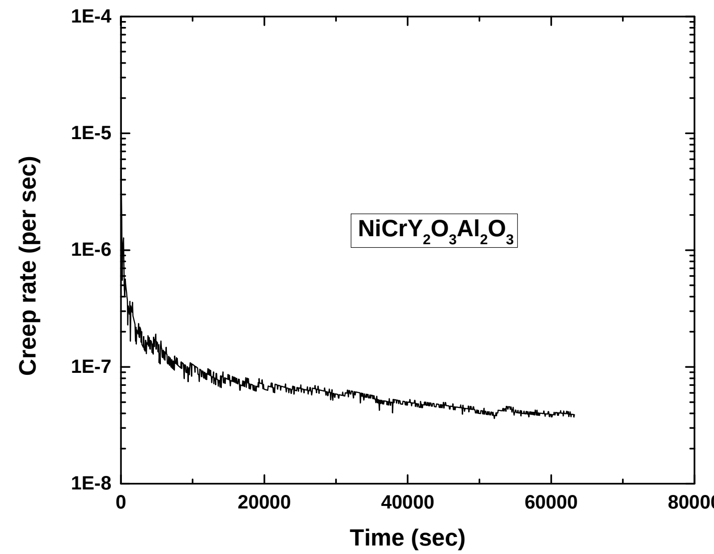

Specimen dimensions (mm*mm*mm)	Stress applied (MPa)	Testing temperature (^oC)
(6.26) * (4.71)* (4.20)	100	800

Minimum creep rate (s^{-1}): $3.7*10^{-8}$

Future Work

- Continue dislocation simulation work
- Complete mechanical property evaluation
- Determine discrepancy between theoretical/computational predictions and experimental results
- Produce guidelines for high temperature microstructural design

Thank You